

SI{97{17

November 1997

HARD DIFFRACTION AND CENTRAL DIFFRACTION IN HADRON{HADRON AND PHOTON{HADRON COLLISIONS

R. Engel[†], University of Delaware, Bartol Research Institute, Newark, DE 19716 USAJ. Ranft[‡], F I G S and Physics Dept. Universitat Siegen, D {57068 Siegen, Germany

Hadron production in single and central diffractive dissociation is studied in a model which includes soft hadron interaction as controlled by a supercritical pomeron parametrization and hard diffractive. Hard diffractive is described using leading-order QCD matrix elements together with the parton distributions for the proton, the less well known photon parton densities and a conjectured parton distribution function for the pomeron. Within this model, particle production in collisions with pomerons exhibit properties like multiple soft interactions and multiple minijets, quite similar to hadron production in non-diffractive hadronic collisions at high energies. However, important differences occur in transverse momentum jet and hadron distributions. It is shown that the model is able to describe data on single diffractive hadron production from the CERN-SPS collider and from the HERA lepton-proton collider as well as first data on central diffractive dissociation. We present also model predictions for single and central diffractive at TEVATRON.

1. Introduction

High-energy hadron production in hadron{hadron collisions and in hadronic interactions of photons is characterized by two mechanisms: (i) minijet production and (ii) soft hadronic interactions. Whereas the minijet cross section can be estimated applying the QCD-improved parton model, soft hadron production cannot be computed directly from perturbative QCD. Most models for multiparticle production being constructed in form of Monte Carlo event generators use soft and hard mechanisms. Such models are usually called minijet models if they use minijets and a simple model for the soft component of the interaction. They are called two component Dual Parton models (DPM's) if they use minijets and incorporate a evolved soft component which is derived from Regge theory, Gribov's reggeon calculus [1,2] and Abramowski-Gribov-Kancheli

(AGK) cutting rules [3] (a review is given in Ref.[4]).

Models inspired by Regge theory or the DPM describe high-mass diffractive hadron production in terms of the so-called triple-pomeron graph. According to this diffractive processes can be considered as collisions of a color neutral object, the pomeron, with hadrons, photons or other pomerons. Experimental data on diffractive support this idea showing that diffractive dissociation exhibits similar features as non-diffractive hadron production whereas the mass of the diffractively produced system corresponds to the collision energy in non-diffractive interactions [5,6]. The striking similarities between diffractive and non-diffractive multiparticle production suggest that multiple soft and hard interactions may also play an important role in high-mass diffractive dissociation.

However the pomeron cannot be considered as an ordinary hadron. It is important to keep in mind that the pomeron is only a theoretical object providing an effective description of the im-

[†]Talk presented by J. Ranft at the International Symposium on Near Beam Physics, Fermilab, 22-24 Sept. 1997

[‡]e-mail: eng@lepton.bartol.udel.edu

[‡]e-mail: Johannes.Ranft@cern.ch

portant degrees of freedom of a certain sum of Feynman diagrams in Regge limit. Pomeron-hadron or pomeron-pomeron interactions can only be discussed in the framework of collisions of other particles like hadrons or photons in terms of single, double or central di-raction dissociation.

The DPM was already successfully applied to di-ractive hadron production reactions [7,9] and even hard di-ractive processes [10]. In [11] cross sections on single and central di-raction were calculated. Up to now, the minijet component in di-ractive processes within the two-component DPM was obtained using a parton distribution function (PDF) for the pomeron and flux factorization. The soft component of di-ractive interactions was described by two hadronic chains (cutting the triple-pomeron graph). Here we will argue, that for the description of di-raction dissociation producing hadronic systems with very large masses, such models are not enough. Also for high-mass di-ractive hadron production we need multiple soft and multiple hard interactions.

2. The Model

2.1. The event generator Phojet

In the Phojet model [12,13], interactions of hadrons are described within the DPM in terms of reggeon (R) and pomeron (P) exchanges. The realization of the DPM with a hard and a soft component is similar to the event generator Dtu-jet [14,15] for $p\bar{p}$ and $p\bar{p}$ collisions. In the following we briefly describe the treatment of the pomeron exchange in non-di-ractive interactions since the same framework is also used for the description of particle production in di-raction dissociation.

The pomeron exchange is artificially subdivided into soft processes and processes with at least one large momentum transfer (hard processes). This allows us to use the predictive power of the QCD-improved Parton Model with lowest-order QCD matrix elements [16,17] and parton density functions. Practically, soft and hard processes are distinguished by applying a transverse momentum cutoff p_T^{cut} to the partons. Consequently, the pomeron is considered as a two-component object with the Bom graph cross sec-

tion for pomeron exchange given by the sum of hard and soft cross sections.

2.2. Di-ractive cross section calculation

Concerning di-raction dissociation, our approach is the following.

In order to get an effective parametrization of Bom graphs describing di-raction within Gribov's reggeon calculus, we calculate the triple-, loop- and double-pomeron graphs using a renormalized pomeron intercept $\alpha_P = 1 + \epsilon_P = 1.08$. For example, let's consider the Bom graph cross sections for high-mass di-raction dissociation in $A\{B$ scattering (for simplicity, we omit in the following expressions the pomeron signature factors; for a discussion of the couplings etc. see [11]).

High-mass single di-raction dissociation of particle A is calculated using the triple-pomeron approximation

$$\frac{d^2 \sigma_{AB}^{TP;A}}{dt dM_D^2} = \frac{1}{16} g_{BP}^0 g_{3P}^0 g_{AP}^0 \frac{s}{s_0} \frac{s_0}{M_D^2} \exp \left[b_{AB}^{SD} t \right] : (1)$$

The differential cross sections for the high-mass double di-raction dissociation reads

$$\frac{d^3 \sigma_{LP}}{dt_1 ds_1 dt_2 ds_2} = \frac{1}{16} g_{AP}^0 g_{3P}^0 g_{BP}^0 \frac{s}{s_0} \frac{s_0}{M_{D1}^2} \frac{s_0}{M_{D2}^2} \exp \left[b_{AB}^{DD} t \right] : (2)$$

Finally, we give the expression for central di-raction dissociation

$$\frac{d \sigma_{DP}}{dt_1 ds_1 dt_2 ds_2} = \frac{1}{256} \frac{1}{s_0^2} (g_{AP}^0 g_{BP}^0 g_{3P}^0)^2 \frac{s}{s_0} \frac{s}{s_1} \frac{s}{s_2} \frac{1}{s_1 s_2} \exp \left[b_A^{CD} t_1 + b_B^{CD} t_2 \right] (3)$$

The experimentally observable di-ractive cross sections (i.e. cross sections of rapidity gap events)

are considerably smaller than the Born graph cross section given in (1), (2) and (3). The reason for this are significant shadowing contributions which are estimated by a two-channel eikonal model [14,13]. It should be emphasized that these shadowing contributions lead to an effective pomeron flux function which is energy as well as projectile and target dependent. Hence the pomeron flux does not obey factorization within this model.

2.3. Particle production in diffractive dissociation

However, not only for cross section calculations, but also for the description of particle production, shadowing effects are important. Unitarity and AGK cutting rules predict that shadowing effects are directly connected with so-called multiple interaction contributions. In the case of diffractive multiparticle production we have to consider rescattering effects in pomeron-hadron and pomeron-pomeron interactions of enhanced graphs. Whereas it was sufficient to introduce a renormalized pomeron trajectory to calculate cross sections, one needs for the calculation of particle production a model for the physical final states which correspond to the unitarity cut of such a renormalized pomeron propagator. Following Refs. [18,19] we assume that the pomeron-pomeron coupling can be described by the formation of an intermediate hadronic system h^2 where the pomerons couple to. Assuming furthermore that this intermediate hadronic system has properties similar to a pion, then the n -m pomeron coupling reads [19]

$$g_{n-m} = G \prod_{i=1}^{n+m-2} g_{h^2 P} \quad (4)$$

with $g_{h^2 P} = g_P$ being the pomeron-pion coupling. G is a scheme-dependent constant. Hence, pomeron-hadron and pomeron-pomeron scattering should exhibit features similar to pion-hadron and pion-pion scattering.

To introduce hard interactions in diffractive dissociation, the exchanged (renormalized) pomerons in pomeron-hadron and pomeron-pomeron scattering are again treated as two-

component objects

$$a_{A P}(s; B) = \frac{i}{2} G \exp \left(\frac{B^2}{4b_P(M_D^2)} \right) \quad (5)$$

with the diffractive eikonal functions

$$\chi_S^{di} = \frac{g_{A P}^0 g_{h^2 P}^0 (M_D^2 = s_0)^P}{8 b_P (M_D^2)} \exp \left(\frac{B^2}{4b_P (M_D^2)} \right) \quad (6)$$

$$\chi_H^{di} = \frac{g_{A P}^{hard} (M_D^2)}{8 b_{h,di}} \exp \left(\frac{B^2}{4b_{h,di}} \right) \quad (7)$$

In all calculations the pomeron PDFs proposed by Capella, Kaidalov, Merino, and Tran (CKMT) [20,21] with a hard gluon component are used.

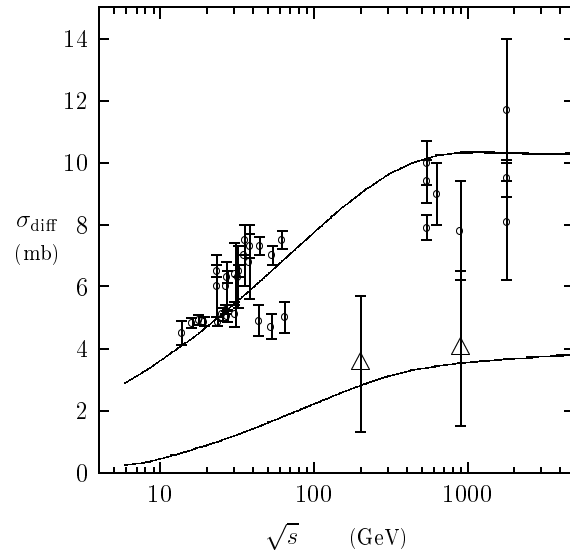


Figure 1. Single and double diffractive pp cross sections as a function of the center of mass energy \sqrt{s} calculated with the model. We compare to data on single diffractive cross sections [22-30]. In addition, some experimental estimates for the cross section on double diffractive dissociation [26,27] are shown.

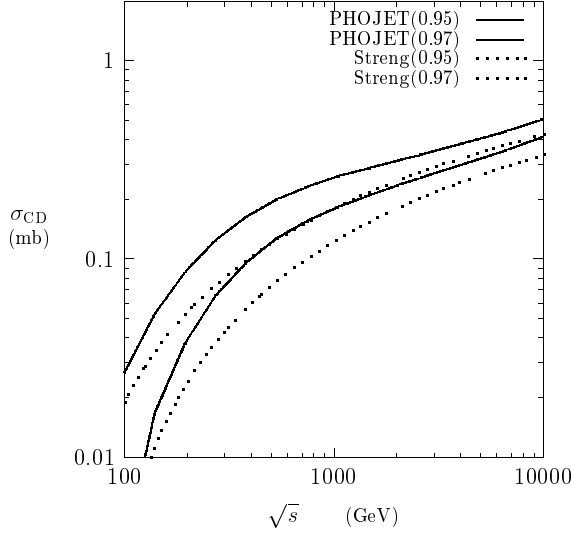


Figure 2. The energy dependence of the central di-raction cross section. We compare the cross section as obtained from Phojet with unitarization using a supercritical pomeron with the cross section obtained by Streng [31] without unitarization and with a critical pomeron. Both cross sections are for the same two kinematic cuts: $M_{CD} > 2 \text{ GeV}/c^2$ and $c = 0.95$ and 0.97 . The cross sections decrease with rising c .

2.4. Toy model with direct pomeron coupling

To estimate the sensitivity of the model results to non-factorizing coherent pomeron contributions as proposed in [32,33], we use optionally also a toy model with a direct pomeron-quark coupling [34]. In this case, the pomeron is treated similar to a photon having a flavor independent quark coupling. For definiteness, the corresponding matrix elements are given

$$\mathcal{M}_{Pq \rightarrow qq}^2 = s \frac{8\hat{u}^2 + \hat{s}^2}{3\hat{s}\hat{u}} \quad (8)$$

$$\mathcal{M}_{Pg \rightarrow qq}^2 = s \frac{\hat{u}^2 + \hat{t}^2}{\hat{t}\hat{u}} \quad (9)$$

$$M_{P \rightarrow qq}^2 = e_q^2 \frac{\hat{u}^2 + \hat{t}^2}{6\hat{u}\hat{t}} \quad (10)$$

$$\mathcal{M}_{Pq \rightarrow qq}^2 = s \frac{\hat{u}^2 + \hat{t}^2}{6\hat{u}\hat{t}} \quad (11)$$

Here, s (e_m) denotes the strong (electromagnetic) coupling and \hat{s} , \hat{t} and \hat{u} are the Mandelstam variables of the partonic scattering process.

3. Comparison with data

3.1. Diffractive cross sections

First we compare single diffractive cross sections according to our model in $p\{p$ collisions to data and we present the results of the model for single and double diffractive cross sections in $\{p$ collisions and for central di-raction cross sections in $p\{p$ collisions. Studying diffractive cross sections is not the primary concern of this paper. Results on diffractive cross sections were already presented using the Dtujet model in Refs. [14,15] and using the present Phojet model in Refs. [12,11], we include updated results for these cross sections here to make the present paper self-contained.

In Fig. 1 data on single diffractive cross sections [22{30] are compared with our model results. It is to be noted that the data on single diffractive cross sections at collider energies are subject to large uncertainties. Nevertheless the rise of the cross section from ISR energies to the energies of the CERN and FERMILAB colliders is less steep than expected from the Born level expression from the triple pomeron formula (1). It is the eikonal unitarization procedure in the model, which suppresses the strong rise of the triple pomeron cross section in the full model. The same effect was also found by Capella et al. [35] and Gotsman et al. [36].

In Fig. 2 we compare as function of the energy the central di-raction cross sections in proton-proton collisions, which we obtain from Phojet with the cross section obtained by Streng [31]. In Phojet we use a supercritical pomeron with $\alpha_P = 0.08$ whereas Streng [31] uses a critical Pomeron with $\alpha_P = 0$. Note that also the double-pomeron cross section grows in Born approximation with s like s^2 . This rapid increase is damped in Phojet by the unitarization procedure. At high energies, contributions from multiple interactions become important. The ra-

pseudorapidity gaps are filled with hadrons due to inelastic rescattering and the cross section for central diffraction gets strongly reduced. In contrast, Streng calculates only the Born term cross section. Figure 2 illustrates the differences obtained using different theoretical methods. We stress, both methods use the measured single diffractive cross sections to extract the triple-pomeron coupling.

3.2. Single diffraction in hadron-hadron collisions at collider energies

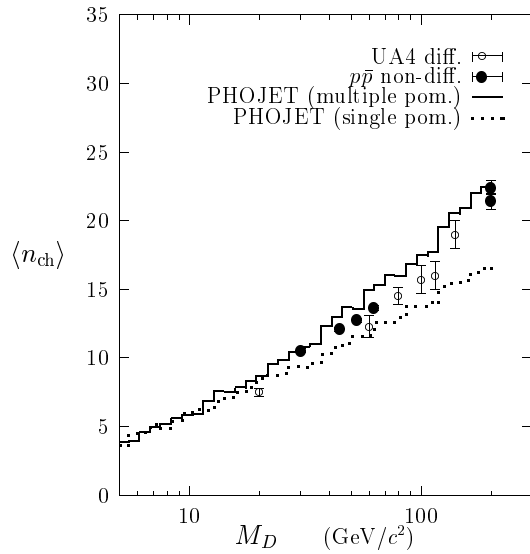


Figure 3. Mean charged particle multiplicity of the diffractively produced hadronic system with invariant mass M_D . UA4 data [6] are compared to single and multiple interaction model predictions and data on non-diffractive pp interactions at $\sqrt{s} = M_D$.

There are the following experiments which have studied hadron production in single diffraction in pp collisions at the CERN SPS/Collider:

1. The UA4 Collaboration [37,6,38] measured pseudorapidity distributions of charged

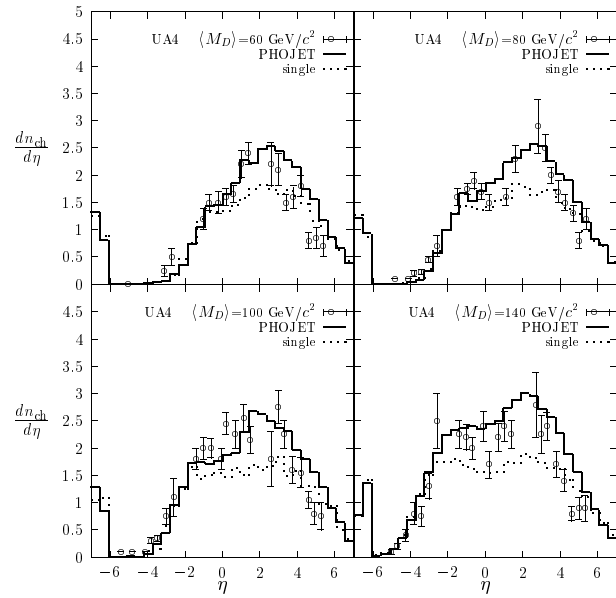


Figure 4. Pseudorapidity distribution of charged hadrons in single diffraction dissociation. UA4 data [6] to model predictions.

hadron production for different masses of the diffractive system. We have already twice compared earlier versions of the Dual Parton Model [8,9] to this data. New in the present model is hard diffraction and multiple chains in the diffractive hadron production, therefore we have again compared to this data and we find reasonable agreement (see Figs. 3 and 4). In particular we present besides the distributions according to the full model also the contribution from one pair of chains only (single interaction model). This is the rapidity distribution expected from the Born term without the contributions from hard diffraction (minijets) and multiple soft interactions, which are obtained from the unitarization method. It is evident from the data as well as from the model that multiple interactions and minijets lead to a rising rapidity plateau in pomeron-proton collisions in a similar way

as observed in hadron-hadron collisions.

- Hard diffractive proton-antiproton interactions were investigated by the UA8 Collaboration [39]. In this experiment the existence of a hard component of diffraction was demonstrated for the first time. Because of the importance of these findings, we compared them already in a recent paper [10] to our model and found the model to be consistent with this experiment. Therefore we will not repeat this comparison here.

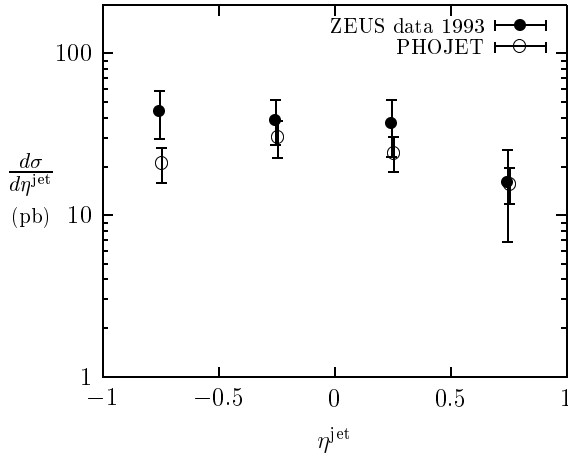


Figure 5. Differential $e-p$ cross section $d\sigma/d\eta^{\text{jet}}(\eta_{\text{max}}^{\text{had}} < 1.8)$ for inclusive jet production with $E_T^{\text{jet}} > 8 \text{ GeV}$ in the kinematic region $Q^2 = 4 \text{ GeV}^2$ and $0.2 < y < 0.85$. We compare data from the ZEUS Collaboration [40] with PhoJet results using the same trigger as used for the ZEUS data.

3.3. Single diffraction in photoproduction

Results on single photon diffraction dissociation and in particular hard single diffraction were presented by both experiments at the HERA electron-proton collider [42, 44, 45, 46].

The ZEUS Collaboration [40] has presented differential and integrated jet pseudorapidity cross

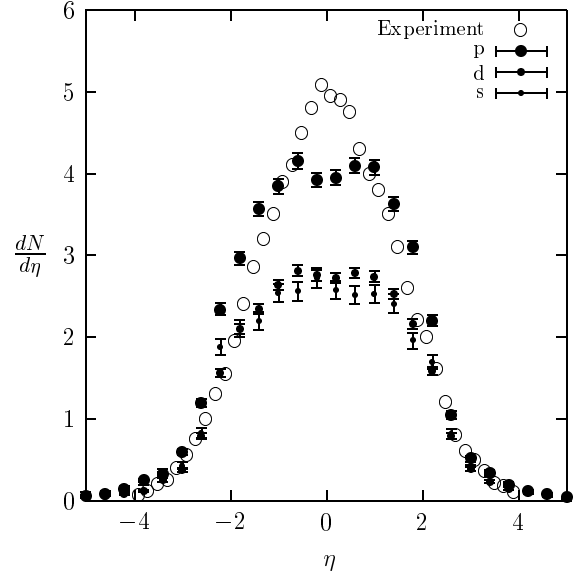


Figure 6. The pseudorapidity distribution in central diffraction as observed by the UA1 Collaboration [41] compared with the corresponding distribution in PhoJet without direct pomeron coupling with the UA1 trigger applied to the Monte Carlo events (p), with a direct pomeron coupling (d) and without multiple interactions (s).

sections for jets with $E_T^{\text{jet}} > 8 \text{ GeV}$. The absolute normalization of these data is given. This allows one a more severe check of the model. In Figs. 5 we compare the differential jet pseudorapidity cross sections from ZEUS [40] to the model. The Monte Carlo events from PhoJet have been treated with the same cuts and trigger as used for the data. We find a reasonable agreement. We should, however, point out that the data include contributions from non-diffractive processes while the results from the model concern only diffractive events.

3.4. Central diffraction dissociation

Data on hard central diffraction in proton-antiproton collisions at 0.63 TeV have been published by Joyce et al. [41]. These data were ob-

tained with the UA1 detector at the CERN SPS collider. The data are not easy to understand since they have been obtained with triggers demanding a pair of jets with $E_t > 3$ GeV or localized electromagnetic energy depositions larger than 1.2 GeV. This trigger accepts a cross section of 0.3 nb while we find in our model at this energy a total central di-radiation cross section of approximately 0.3 mb (see Fig. 2). Thus the trigger of Joyce et al. [41] accepts only a tiny fraction of all central di-radiation events. The most remarkable features of the data are the following:

The pseudorapidity distribution of the events accepted by the trigger reaches a maximum central plateau of around 5 per pseudorapidity unit, 30 percent higher than the non-diffractive minimum bias events at the full p-p collision energy.

We try to understand these data [41] in three versions of the model. (i) The full model without a direct pomeron coupling, (ii) the full model with a direct pomeron quark coupling, (iii) the model without multiple interactions and without a direct pomeron coupling. We use for the Monte Carlo events the same trigger requirements as described in [41].

In Fig. 6 the charged particle distribution of the three versions of the model are compared to the data. Only the full model gives a pseudorapidity maximum comparable to the data. This is easy to understand, only in the full model we have enough multiple soft chains and multiple minijets to obtain such a large particle density. In the model without multiple interactions and without a direct pomeron coupling we trigger to events with one pair of direct jets, this does not give enough particle density. Similarly in the model without multiple interactions we just get one pair of soft chains together with a minijet, also in this configuration the particle density is lower than in the full model.

4. Comparing hadron production in diffractive processes to non-diffractive particle production in p-p and p-p collisions

In Sections II we have already pointed out, that our model for particle production in pomeron-hadron/photon collisions and pomeron-pomeron

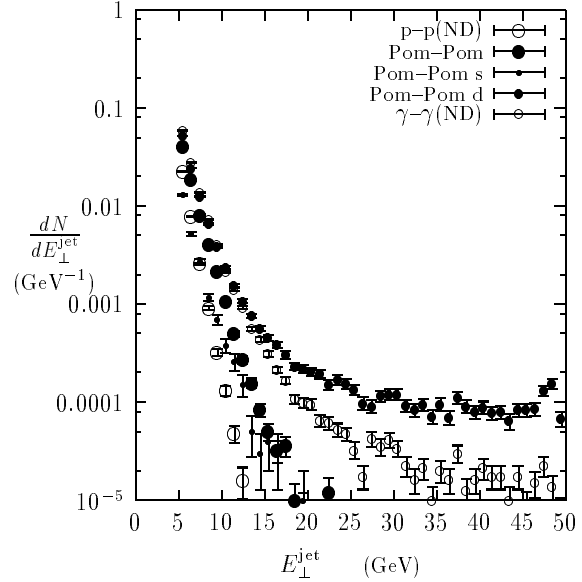


Figure 7. Jet transverse energy distributions in non-diffractive p-p and p-p collisions compared with the jet transverse energy distribution in central di-radiation (pomeron-pomeron collisions). For the latter channel we give the distributions separately for the full model, the model without multiple interactions (s) and the model with a direct pomeron coupling (d). The distributions were generated with PHOJET, the c.m. energy / diffractive mass is 100 GeV in all cases.

collisions has the same structure characterized by multiple soft collisions and multiple minijets like models for hadron production in hadron-hadron collisions. Therefore, again we expect the main differences in comparison to other channels in the hard component due to the differences between the pomeron and hadron structure functions and due to the existence or nonexistence of a direct pomeron-quark coupling. We will use in all comparisons here three models for P-p, P-p and P-P collisions:

- (i) our model with multiple soft and hard collisions,
- (ii) in order to see the influence of the multiple soft and hard collisions a model with only one soft

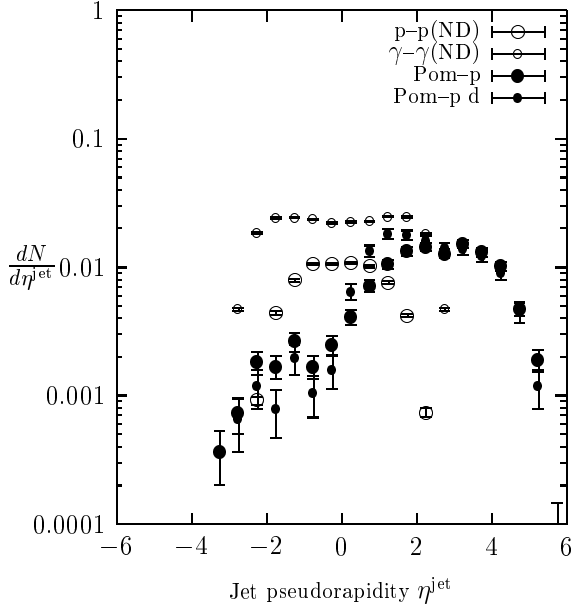


Figure 8. Jet pseudorapidity distributions in non-diffractive $p\{p$ and $\{\gamma\gamma$ collisions compared with the jet pseudorapidity distribution in single diffractive (pomeron $\{p$ scattering). The distributions were generated with Phojet, the c.m. energy is 100 GeV in all cases, but the pseudorapidity in the collisions with pomerons given refer to the $\sqrt{s} = 2$ TeV $p\{p$ collisions used to generate the diffractive events.

or hard collision allowed and

(iii) the full model (i) assuming in addition the existence of a direct pomeron $\{quark$ coupling according to the toy model. We present this despite the fact that we did not find in the presently existing data any feature which could only be described with such a coupling.

The differences in the parton structure functions of protons, photons and pomerons lead to quite different energy dependences of the hard cross sections. In all processes where pomerons are involved, single diffractive and central diffractive, hard processes become important already at lower energies. For pomeron $\{pomeron$ scattering at low energy the hard cross section is about a fac-

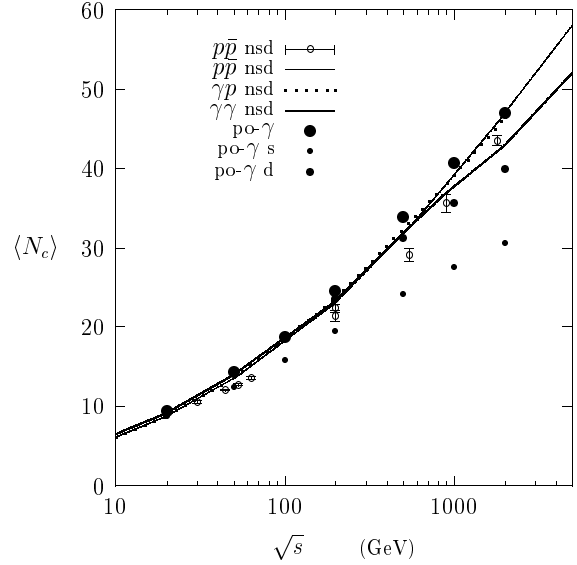


Figure 9. Average charged multiplicity as function of the c.m. energy in single diffractive collisions (pomeron $\{ collisions) according to Phojet (points) is compared to the average charged multiplicities in non single diffractive pp , p and $\gamma\gamma$ collisions, also according to Phojet (lines) and experimental data in pp collisions.$

tor 100 bigger than in $p\{p$ collisions. At high energies the opposite happens, the hard cross sections in all processes where pomerons are involved rise less steep with the energy than in pure hadronic or photonic processes. The reason for this is the different low- x behavior of the parametrization of the structure functions used. However, nothing is known at present from experiment about the low- x behavior of the pomeron structure function.

In Fig. 7 we compare jet transverse energy distributions in $p\{p$ and $\{\gamma\gamma$ collisions with the ones in $P\{P$ collisions. In the channels with pomerons we present again the distributions according to our full model, according to the model without multiple interactions and the model with a direct pomeron $\{quark$ coupling. In all non-diffractive collisions we have $\sqrt{s} = 100$ GeV and the diffractive events are generated in $\sqrt{s} = 2$ TeV collisions

with $M_D = 100 \text{ GeV}$. The differences in the jet transverse energy distributions between the channels are as to be expected more important than in the hadron p_T distributions. We observe an important reduction in the jet distributions in the model without multiple interactions. The effect of the direct pomeron coupling is as dramatic as the effect due to the direct photon coupling. The E_T distributions in the $P\{$ and $P\{P$ channels extend up to the kinematic boundary. In the latter two cases as in the case of $\{$ collisions the entries at large E_T come only from direct processes.

In Fig. 8 we compare jet pseudorapidity distributions in $p\{p$, $\{$ and $P\{p$, again, all collisions at $\sqrt{s} = 100 \text{ GeV}$ with the diffractive events generated in $\sqrt{s} = 2 \text{ TeV}$ collisions. For the jets we observe substantial differences in the shape of the pseudorapidity distributions.

In Figs. 9 we compare the average charged multiplicity in non-diffractive $p\{p$, $\{$ and $\{p$ collisions according to the model as function of \sqrt{s} with the charged multiplicity in the pomeron{diffractive channel as function of the invariant mass of the diffractive system.

In the same plots we compare also to data in the case of $p\{p$ collisions. We end at collision energies below say 500 GeV only small differences between the channels. However, at energies above 1 TeV the model with only one pomeron exchange (one-pomeron cut) in diffractive dissociation (labeled with s) predicts a smaller average multiplicity than observed in hadron-hadron or photon-hadron scattering.

5. Single diffractive and central diffractive at TEVATRON

In Figs. 10 to 17 we present some cross sections calculated using Phojet at TEVATRON energy. The distributions are mass distributions in single and central diffractive Fig. 10, jet pseudorapidity distributions in single and central diffractive as well as in non-diffractive $p\{p$ collisions (ND) using E_T thresholds of 5 and 15 GeV Fig. 11 to 13, Jet E_T distributions Fig. 14 to 16 and the charged multiplicity as function of the diffractive mass Fig. 17. In some of the distributions we give besides the full Phojet model also the plots for a

model with a small direct pomeron coupling and for a model with only single soft or hard chains pairs.

Results on diffractive jet production from the two TEVATRON Collaborations are discussed in [47{51], one of the results obtained by the D0 Collaboration is the ratio of double{pomeron exchange (DPE) (in the present paper we use the term central diffractive (CD) instead of DPE) to non{diffractive (ND) dijet events:

$$\frac{(DPE)}{(ND)} \Big|_{E_T^{\text{jet}} > 15 \text{ GeV}} \approx 10^{-6} \quad (12)$$

Phojet gives the following cross sections:

Non-diffractive (ND): $(ND) = 45.2 \text{ mb}$,

Single diffractive (SD): $(SD) = 11.2 \text{ mb}$,

Central diffractive (CD): $(CD) = 0.64 \text{ mb}$.

From these cross sections together with Figs. 11 to 16 we get for this and similar ratios always for E_T larger than 15 GeV :

$$\begin{aligned} (CD)/(ND) &\approx 2 \cdot 10^{-6}, \\ (SD)/(ND) &\approx 4 \cdot 10^{-3}, \\ (CD)/(SD) &\approx 0.5 \cdot 10^{-3}. \end{aligned}$$

Despite the fact that no experimental acceptance has been considered for these Phojet results it is interesting to find the $(CD)/(ND)$ ratio so close to the D0 value given above.

6. Conclusions and summary

Multiple soft and multiple hard interactions (minijets) have been introduced to describe high-mass diffractive hadron production. Comparing diffractive dissociation with the invariant mass M_D to non-diffractive particle production at $M = \sqrt{s}$, a rise of the rapidity plateau and multiplicity is found which is similar for both hadron production processes. The model predictions agree well with data on high-mass single and central diffractive dissociation.

Minimum bias hadron production in hadron-hadron, and photon-photon collisions as well as in pomeron{hadron, pomeron{photon and pomeron{pomeron collisions of the same cm. energy is remarkably similar. To see this, one has to restrict the comparison to inelastic events and to exclude also the diffractively produced vector mesons in reactions involving photons. The only

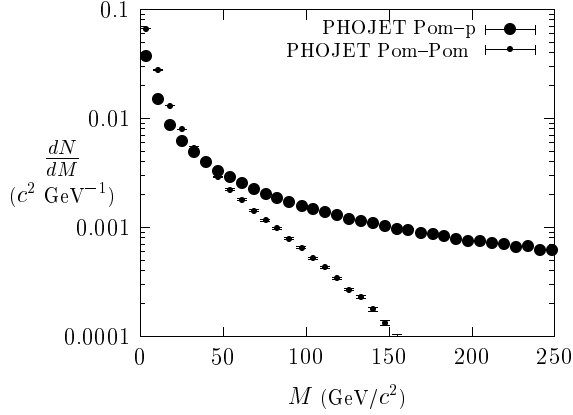


Figure 10. Distribution of the diffractive mass in single diffraction (Pomeron{proton}) and central diffraction (Pomeron{Pomeron}) at TEVATRON with $\sqrt{s} = 1.8$ TeV.

striking differences appear in the transverse momentum distribution or distributions where the transverse momentum behavior is essential. This difference can be understood to be due to the direct photon interaction contribution and due to the photon and pomeron structure functions being considerably harder than hadronic structure functions.

Finally we would like to emphasize that measurements at TEVATRON on CD and SD would allow one to study many of the open questions: Is it possible at all to describe diffraction and hard diffraction using the triple pomeron graph? Can QCD factorization be applied to the description of hard diffraction? Does a direct pomeron{quark coupling exist? Do we have multiple soft and hard chains in diffractive particle production?

Acknowledgments

The authors are grateful to F.W. Bopp and S. Roesler for many discussions. One author (R.E.) thanks T.K. Gaisser for helpful comments and remarks. The work of R.E. is supported in part by the U.S. Department of Energy under Grant DE-FG 02-91ER 40626.

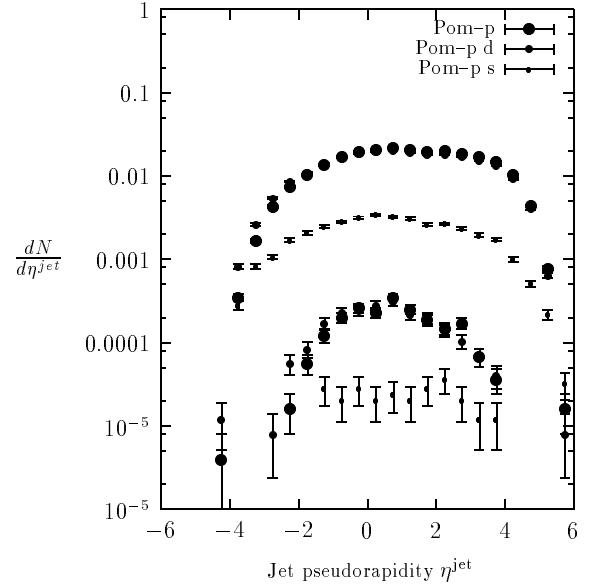


Figure 11. Pseudorapidity distribution of jets with E_T larger than 5 GeV and 15 GeV in (one side) single diffraction (Pom{p}) at TEVATRON. The upper curves with the same plotting symbol are generally for $E_T = 5$ GeV, the lower curves are for $E_T = 15$ GeV. We plot also the distributions (d) using a small direct Pomeron coupling ($\alpha = 0.05$) and (s) in a model where only single soft or hard chains are permitted.

REFERENCES

1. V.N. Gribov: Sov. Phys. JETP 26 (1968) 414
2. V.N. Gribov and A.A. Migdal: Sov. J. Nucl. Phys. 8 (1969) 583
3. V.A. Abramovski, V.N. Gribov and O.V. Kancheli: Sov. J. Nucl. Phys. 18 (1974) 308
4. A. Capella, U. Sukhatme, C. I. Tan and J. Tr  n Thanh V  n: Phys. Rep. 236 (1994) 225
5. K. Goulianos: Phys. Rep. 101 (1983) 169
6. UA4 Collab.: D. Bernard et al.: Phys. Lett. B 166 (1986) 459
7. V. Innocente, A. Capella, A.V. Ramello and J. Tr  n Thanh V  n: Phys. Lett. B 169 (1986)

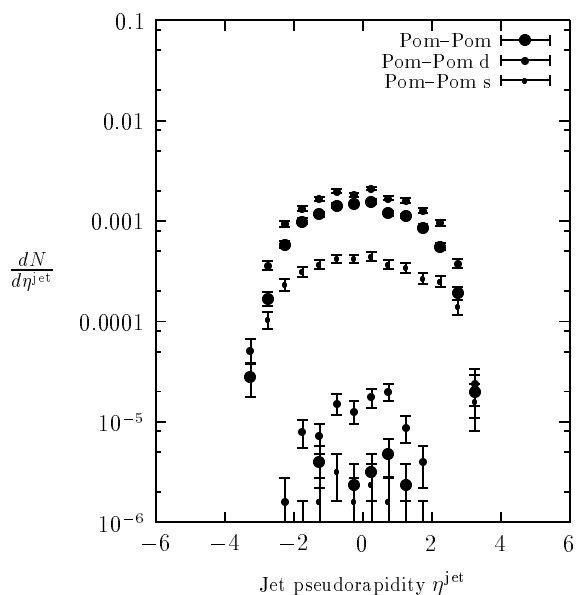


Figure 12. Pseudorapidity distribution of jets with E_T larger than 5 GeV and 15 GeV in central di-rapion (Pom-Pom) at TEVATRON. The upper curves with the same plotting symbol are for $E_T = 5$ GeV, the lower curves are for $E_T = 15$ GeV. We plot also the distributions (d) using a small direct Pomeron coupling ($\alpha = 0.05$) and (s) in a model where only single soft or hard chains are generated.

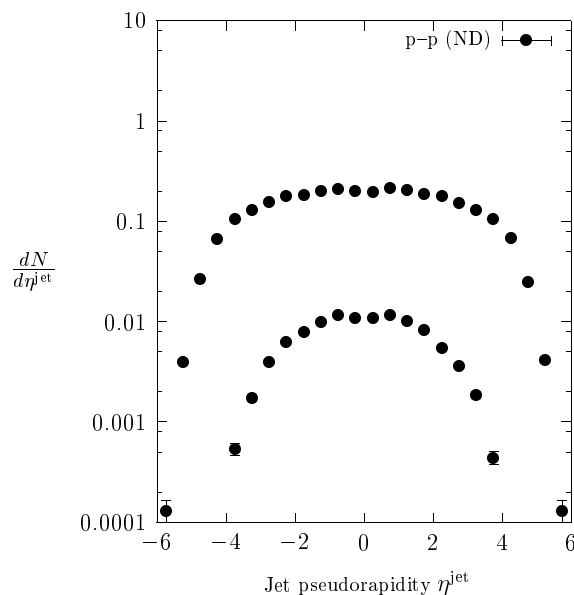


Figure 13. Pseudorapidity distribution of jets with E_T larger than 5 GeV and 15 GeV in non-diffractive (ND) p-p collisions at TEVATRON. The upper curve is for $E_T = 5$ GeV and the lower curve is for $E_T = 15$ GeV.

- 285
8. J. Ranft: Z. Phys. C 33 (1987) 517
 9. S. Roesler, R. Engel and J. Ranft: Z. Phys. C 59 (1993) 481
 10. R. Engel, J. Ranft and S. Roesler: Phys. Rev. D 52 (1995) 1459
 11. R. Engel, M. A. Braun, C. Pajares and J. Ranft: Z. Phys. C 74 (1997) 687
 12. R. Engel: Z. Phys. C 66 (1995) 203
 13. R. Engel and J. Ranft: Phys. Rev. D 54 (1996) 4244
 14. P. Aurenche, F. W. Bopp, A. Capella, J. Kwiecinski, M. Maire, J. Ranft and J. Tran Thanh Van: Phys. Rev. D 45 (1992) 92
 15. F. W. Bopp, R. Engel, D. Pertemann and

- J. Ranft: Phys. Rev. D 49 (1994) 3236
16. B. L. Combridge, J. Kwiecinski and J. Ranft: Phys. Lett. B 70 (1977) 234
17. D. W. Duke and J. F. Owens: Phys. Rev. D 26 (1982) 1600
18. J. L. Cardy: Nucl. Phys. B 75 (1974) 413
19. A. B. Kaidalov, L. A. Ponomarev and K. A. Ter-Martirosyan: Sov. J. Nucl. Phys. 44 (1986) 468
20. A. Capella, A. Kaidalov, C. Merino and J. Tran Thanh Van: Phys. Lett. B 343 (1995) 403
21. A. Capella, A. Kaidalov, C. Merino, D. Pertemann and J. Tran Thanh Van: Phys. Rev. D 53 (1996) 2309
22. J. W. Chapman et al.: Phys. Rev. Lett. 32 (1974) 257
23. J. Schamberger et al.: Phys. Rev. Lett. 34 (1975) 1121

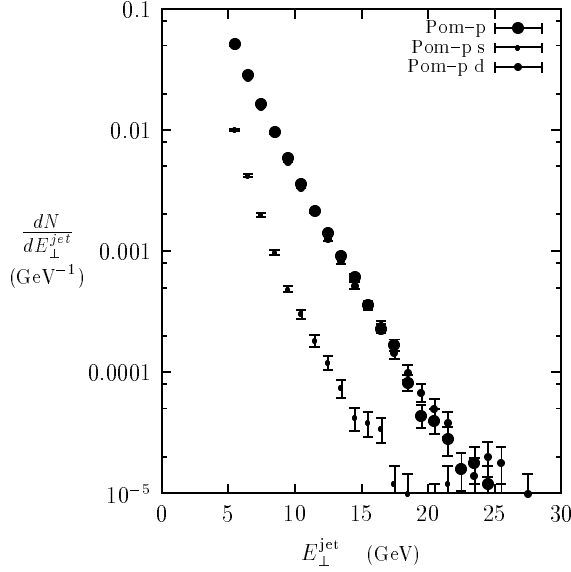


Figure 14. Transverse energy distribution of jets in (one side) single diffraction (Pom {p}) at TEVATRON. We plot also the distributions (d) using a small direct Pomeron coupling ($\alpha = 0.05$) and (s) in a model where only single soft or hard chains are generated.

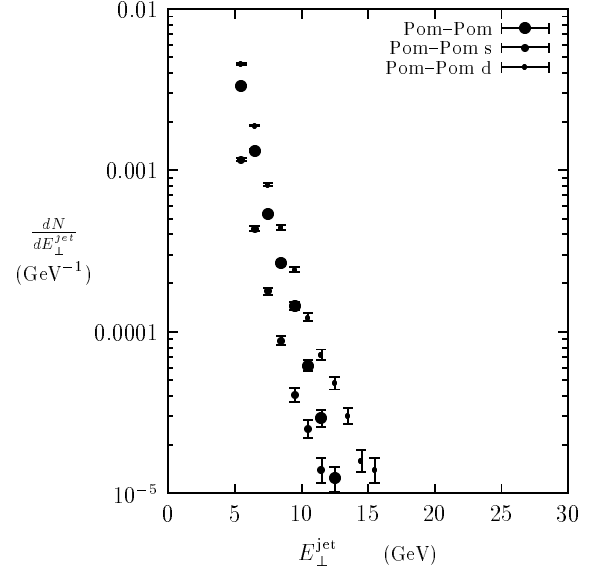


Figure 15. Transverse energy distribution of jets in central diffraction (Pom {Pom}) at TEVATRON. We plot also the distributions (d) using a small direct Pomeron coupling ($\alpha = 0.05$) and (s) in a model where only single soft or hard chains are permitted.

24. CHLM Collab.: M. G. Albrow et al.: Nucl. Phys. B108 (1976) 1
 25. CHLM Collab.: J. C. M. Amstutz et al.: Nucl. Phys. B194 (1982) 365
 26. UA5 Collab.: R. E. Ansorge et al.: Z. Phys. C33 (1986) 175
 27. UA1 Collab.: D. Robinson and C. E. Wulz: Calibration of the UA1 luminosity monitor, Report UA1-TN / 89-10, 1989
 28. E710 Collab.: N. A. Amos et al.: Phys. Lett. B243 (1990) 158
 29. E710 Collab.: N. A. Amos et al.: Phys. Lett. B301 (1993) 313
 30. CDF Collab.: F. Abe et al.: Phys. Rev. D50 (1994) 5535
 31. K. H. Streng: Phys. Lett. 166B (1986) 443
 32. J. Collins, L. Frankfurt and M. Strikman: Phys. Lett. B307 (1993) 161
 33. J. C. Collins, J. Huston, J. Pumplin,

H. Weerts and J. J. Whitmore: Phys. Rev. D51 (1995) 3182
 34. B. Kniehl, H.-G. Kührs and G. Kramer: Z. Phys. C65 (1995) 657
 35. A. Capella, J. Kaplan and J. Trần Thanh Vân: Nucl. Phys. B105 (1976) 333
 36. E. Gotsman, E. M. Levin and U. M. Soffer: Phys. Lett. B353 (1995) 526
 37. UA4 Collab.: M. Bozzo et al.: Phys. Lett. B147 (1984) 392
 38. UA4 Collab.: D. Bernard et al.: Phys. Lett. B186 (1987) 227
 39. UA8 Collab.: A. Brandt et al.: Phys. Lett. B297 (1992) 417
 40. ZEUS Collab.: M. Derrick et al.: Phys. Lett. B356 (1995) 129
 41. D. Joyce et al.: Phys. Rev. D48 (1993) 1943
 42. H1 Collab.: T. Ahmed et al.: Nucl. Phys.

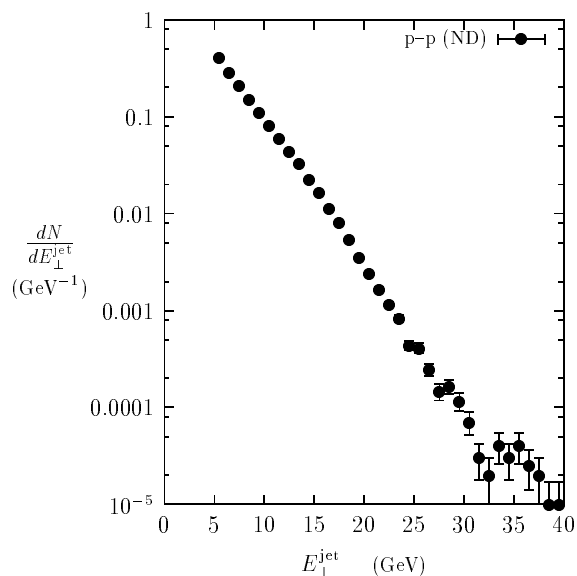


Figure 16. Transverse energy distribution of jets in non-diffractive (ND) p-p collisions at TEVATRON.

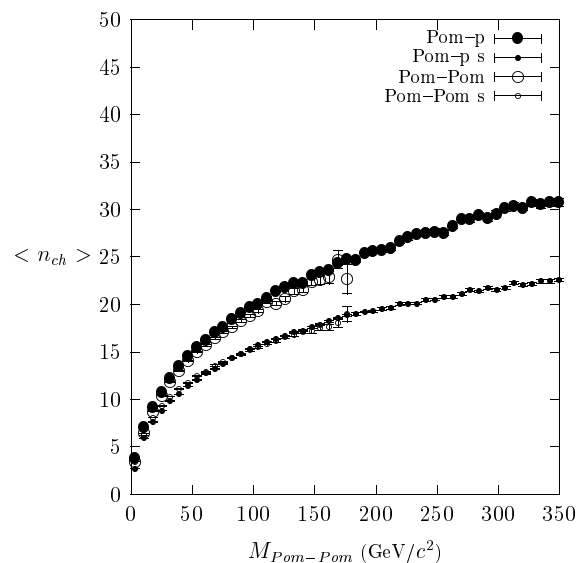


Figure 17. Charged multiplicity as function of the diffractive mass in single diffractive (Pom-p) and central diffractive (Pom-Pom) at TEVATRON. We plot also the distributions (s) in a model where only single soft or hard chains are considered.

B435 (1995) 3

43. H1 Collab.: S. Aid et al.: Z. Phys. C 69 (1995) 27

44. ZEUS Collab.: M. Derrick et al.: Phys. Lett. B 346 (1995) 399

45. ZEUS Collab.: M. Derrick et al.: Z. Phys. C 67 (1995) 227

46. ZEUS Collab.: M. Derrick et al.: High-E_T jet cross sections in photoproduction at HERA, preprint pa02-041, to appear in Proceedings of the XXV III International Conference on High Energy Physics, Warsaw, Poland, 1996

47. M. Albrow: presented at this meeting, 1997

48. A. Brandt: presented at this meeting, 1997

49. A. Santoro: Diffractive phenomena at Tevatron, to be published in the Proceedings of the VI Conference on the Intersection of Particle and Nuclear physics, Big Sky, Montana, USA, 1997

50. K. Goulianos: Results on Diffractive, presented at the XVII th International Conference on Physics in Collision, Bristol, UK,

1997

51. A. Brandt: Rapidity gaps in jet events at D0, to be published in the Proceedings of the XI Topical Workshop on Proton-Antiproton Collider Physics, Albano Terme, Italy, 1996